QI driven processing to enhance the fidelity in a deepwater field

Indranil Samanta[1], Yannick Cobo [1], Darrell Armentrout [1], Rodolfo Hernandez[1], Tiago Alcantara[1], Aurora Rodriguez-Castelan [1], Ika Novianti[1], Khaled Abdelaziz[1], Mohammed Hegazy[1], Qingsong Li[2], Caoana Williams[2], Dhananjay Kumar[2]*
TGS[1], bp[2]

Summary

Broadband seismic data is fundamental to achieving reliable imaging and quantitative interpretation in complex deepwater environments. However, true broadband recovery requires more than extending the frequency spectrum; it demands a carefully designed processing workflow that preserves amplitude, stabilizes wavelets, and controls spatial consistency across offsets and azimuths. This paper presents careful application of a comprehensive wide azimuth (WAZ) broadband reprocessing strategy applied to the deepwater field, leveraging multiple orthogonal wide-azimuth surveys acquired with differing acquisition philosophies.

The workflow integrates early-stage signal conditioning, joint source–receiver deghosting using 3D sparse τ–p inversion (Wang *et. al.,* 2015)., amplitude-preserving demultiple strategies, and survey-specific optimized 3D Offset Vector Tile (OVT) regularization. Special attention is given to minimizing tuning effects, protecting amplitude varying with offset (AVO) behavior, and managing cross-survey information flow through rank-based regularization and masking. Imaging was performed using TTI Wave-equation Kirchhoff pre-stack depth migration (WE-KPSDM) with a merged anisotropic velocity model. Post-imaging enhancements, including AVO guided curvelet co-denoise, high-resolution Radon demultiple, trim statics, and carefully calibrated Q amplitude compensation, further refined the dataset.

The resulting seismic volumes exhibit improved spectral balance, enhanced spatial uniformity, and robust amplitude behavior across offsets and azimuths. This study demonstrates that a quantitative interpretation (QI) -driven broadband processing philosophy focused on fidelity rather than aggressive bandwidth enhancement can deliver seismic data suitable for advanced interpretation and reservoir characterization in challenging deepwater settings.

Introduction

The study area has been covered by multiple wide-azimuth seismic surveys acquired with differing acquisition philosophies and geometries. The two primary WAZ surveys discussed in this study are Justice and Declaration, which are orthogonal in their acquisition orientations. Justice was acquired following a WATS (Regone, 2006) design philosophy, while Declaration was acquired as a StagSeis (Mandroux *et. al.*, 2013) survey with a different sail line orientation and coverage pattern. These complementary, yet dissimilar acquisition geometries present both opportunities and challenges.

Achieving a broadband seismic response that is both high-resolution and amplitude-preserving is critical for reliable reservoir characterization and QI. In complex deepwater settings such as for the field area considered here, the challenge extends beyond bandwidth recovery to ensuring spectral stability, spatial consistency, and true-amplitude fidelity throughout the processing sequence. To address this, the wide-azimuth datasets were reprocessed through a carefully structured workflow designed to restore bandwidth, attenuate noise and multiples, and generate QI-ready products. Band-limited migration QC was embedded throughout the workflow to validate parameter selection and safeguard AVO integrity.

Seismic bandwidth underpins both vertical resolution and inversion reliability. High frequencies improve reflector separation and sharpen thin-bed features, while low frequencies are critical for stabilizing impedance inversion and capturing the correct low-frequency trends. However, true broadband content is often compromised by ghost interference, limited migration aperture, noise contamination, and overly complex processing workflows that can appear visually improved while degrading amplitude fidelity and quantitative reliability. Therefore, the reprocessing workflow must be carefully engineered to restore spectral balance, reduce tuning effects, preserve true amplitudes and enhance continuity.

Successful broadband processing requires the integration of several key elements: accurate estimation and recovery of the effective source signature through optimal designature and deghosting, inelastic attenuation compensation, high signal-to-noise, proper target illumination, dense spatial sampling, accurate velocity modeling, and high-fidelity pre- and post-stack signal processing together with imaging technique that better position the structure. Each of these components was addressed systematically in the dataset considered in this reprocessing effort, beginning with signal conditioning, designature, demultiple, regularization and culminating in advanced imaging algorithm and post-image enhancement workflows. The following sections describe each of these processing steps in detail.

Pre-Deghosting Conditioning

To prepare the data for effective deghosting and broadband recovery, early-stage conditioning was applied to suppress acquisition-related noise and stabilize the wavelet. This included targeted denoise strategies and the application of a statistically robust gun dependent 1D debubble operator derived from limited-offset data (approximately 1 km in the shooting direction), ensured operator stability. Shot-by-shot debubbling was evaluated but not adopted, as those operators proved less stable and less suitable for the AVO objectives compared to the simplified limited-offset stacking approach. This was followed by correction for receiver motion and addressing water-column statics. Together, these steps improved signal-to-noise ratio and waveform stability, providing a clean and consistent input for subsequent designature.

Joint Source-Receiver Deghosting via 3D Sparse τ–p Inversion

The deghosting process was designed to eliminate the spectral notches, phase distortion, and amplitude imbalance introduced by source and receiver ghost reflections off the sea surface (Wang *et. al.*, 2015). A 3D Sparse τ–p inversion based deghosting technique was employed to jointly remove both source- and receiver-side ghost energy. The use of sparsity in the τ–p domain enhances the separation of coherent primaries from overlapping ghost energy while mitigating spatial aliasing due to large cable separations. This method supports angle-dependent deghosting across all azimuths, restoring the full spectral content of the wavelet. Post-deghosting analysis showed improved spectral balance, enhanced phase stability, and greater reflector continuity, establishing a reliable foundation for further processes such as, demultiple, regularization and imaging with a simpler wavelet to start with. Post-deghost debubbling was intentionally not applied, as the residual bubble energy originally appearing as asymmetric sidelobes is redistributed by the zero-phasing effect. This process naturally balances and reduces the bubble imprint, making additional debubbling unnecessary and avoiding potential degradation of the broadband wavelet.

Demultiple

Following deghosting, surface-related multiples were attenuated using a hybrid matching and subtraction strategy built upon an already fine-tuned and globally matched SRME model. Rather than applying aggressive subtraction, mild adaptive matching and subtraction were performed in both highly resolved low frequency curvelet scales and the *x-t* domain. This approach enabled effective suppression of multiple energy while preserving primary amplitudes and AVO behavior.

While attenuation of ghosts and multiple energy can help unmask underlying events of interest in the reservoir window, it also carries the risk of distorting true AVO trends or compromising amplitude integrity if not carefully parameterized (shown in Figure 1a and 1b). To manage this trade-off, all parameter selection and optimization were guided by rigorous image QC and QI interpretation ensuring that primary reflections and amplitude behavior were preserved. Despite effective multiple attenuation, a significant level of residual multiple energy was expected to remain at this stage due to acquisition sampling limitations and the absence of full spatial regularization.

3D Offset Vector Tile (OVT) Regularization was implemented independently for each survey to standardize spatial and azimuthal sampling. Justice WAZ was defined as the Rank-1 reference survey. It had fewer acquisition holes and benefited from a complementary NAZ survey (EMC3D) that provided better coverage. EMC3D and Declaration were designated as Rank-2 and Rank-3, respectively. In contrast to Justice, the Declaration WAZ survey suffered from a large swath of missing coverage with only sparse, randomly distributed traces in few areas. In this context, "rank" denotes the priority assignment during OVT reconstruction.

Justice WAZ was initially regularized using a Matching Pursuit–based inversion to reconstruct missing traces within each OVT tile, with the EMC3D survey providing supplementary coverage to help infill selected areas with acquisition gaps. This regularized output from Justice WAZ was then used to help fill in missing areas in Declaration. However, this created a risk of overfitting Declaration to resemble Justice. In some locations, excessive and uncontrolled mixing led to degradation of valid Rank-3 information. To mitigate this, a system of mask files was introduced to guide where data from Justice could contribute, thereby preserving the native geological characteristics of Declaration. In addition, reciprocal OVT generation was implemented for Declaration, simulating mirrored geometry through reciprocity principles to better populate systematically missing patches in the OVT tiles (shown in Figure 2a and 2b). Together, these strategies significantly improved the spatial uniformity, azimuthal balance, and AVO integrity of the image gathers post regularization and enabling seamless structural image.

Residual demultiple in fine sampled OVT domain

Following 3D OVT regularization, the surface-related multiple models already generated during SRME stage passed through the same OVT regularization workflow to ensure consistency with the input data. This allowed the regularized multiple models to be better matched to the input regularized gathers. Adaptive matching and subtle subtraction were then performed in the OVT domain using this updated multiple models. This step effectively removed a significant portion of high-frequency residual multiple energy that was overlaying reservoir reflections. Leveraging the enhanced spatial sampling and azimuthal uniformity provided by OVT regularization, this step delivered a more coherent pre-stack input for imaging and improved the final image quality by minimizing residual multiple contamination near the reservoir interval.

TTI Wave-Equation Kirchhoff Pre-Stack Depth Migration (WE-KPSDM) was employed for Pre-Stack Depth Migration. WE-KPSDM selected over ray-traced approaches due to its improved handling of multipathing, steep dips, and complex anisotropic velocity regimes typical of deepwater Gulf of Mexico setting. In contrast to ray-based methods that rely on single-arrival approximations, WE-KPSDM numerically solves the wave equation, allowing more accurate treatment of wave phenomena in heterogeneous and anisotropic media (Etgen, 2012; Pu *et. al.,* 2021).

The WAZ surveys were migrated independently using a 8.5 km half-aperture, with input provided by 3D OVT-regularized gathers after application of inverse phase Q compensation prior to imaging. Final stacking and angle-gather generation were carried out on a 25 m × 25 m grid, producing angle stacks suitable for robust AVO analysis.

Post-Imaging Enhancements To enhance interpretability and preserve quantitative integrity, an AVO-consistent post-image processing sequence was implemented. Curvelet-domain co-denoising was applied with a three-term Shuey AVO model used as a reference to guide parameter selection. The AVO response was not imposed on the data but served as a QC framework to ensure that attenuation of noise and residual multiple energy did not impact primary reflections or amplitude trends. This approach was particularly effective in suppressing noise contaminating the reservoir interval and residual multiples with limited moveout separation from primaries, especially at near offsets where Radon-based demultiple methods often struggle or risk primary attenuation. Radon parameterization and multiple models were cross validated against the Shuey's 3 term AVO response to confirm preservation of primary amplitude behavior and reflector continuity. Trim statics were treated as a critical step, as accurate alignment of subtle reflection events has a direct and significant impact on AVO trend interpretation. Residual timing errors in the image gathers were corrected using trim statics derived from cross-correlation against a stacked pilot volume, improving event alignment, gather flatness, and amplitude consistency. This correction was essential to stabilizing AVO behavior and ensuring reliable classification within the reservoir interval.

Inverse Q Filtering, Amplitude Only Q compensation proved to be a sensitive and critical step. A range of Q values was tested to balance spectral enhancement and amplitude fidelity. Lower Q values (Q=100), while addressing stronger attenuation and boosting higher frequencies, were found to degrade AVO behavior and distort the low-frequency content that is essential for quantitative interpretation. Higher Q values (Q=150) preserved AVO trends but provided limited bandwidth recovery at the high frequency end. An optimal compromise was achieved with a Q value of 120, which delivered a balanced broadband response, enhancing high-frequency resolution while maintaining the low-frequency integrity required for both structural interpretation and QI objectives.

Results

Figure 3a presents the legacy least-squares WE-KPSDM image. Figure 3b shows the corresponding image generated using the merged velocity model, producing a structurally continuous result and representing the raw WE-KPSDM output. The updated image exhibits improved low-frequency content and clearer fault definition.

Figures 3c and 3d illustrate the impact with Q = 150 and Q = 120, respectively. Progressive spectral enhancement is observed, with improved reflector clarity at the reservoir level while maintaining AVO integrity. The Q = 120 result provides the flattest and broadest bandwidth relative to the legacy image. In the spectral comparison (Figure 3e), purple denotes the legacy data, green the raw WE-KPSDM result, red the Q = 150 result, and blue the Q = 120 result.

Figure 3f shows AVO-consistency QC across the processing stages. From left to right: the raw image gathers, the post-processed gathers, and the synthetic gathers generated from well data. The post-processed gather exhibits improved signal-to-noise and reflector continuity while maintaining the amplitude-versus-angle behavior observed in the raw data. The AVO trend plot compares raw (red), post-processed (blue), and synthetic (yellow) responses, confirming preservation of the Class III AVO signature within the reservoir window. This gather-plus-AVO QC was performed at key stages to ensure that S/N enhancement did not distort amplitude trends.

Conclusions

The broadband reprocessing effort presented in this study demonstrates that the success of the high-quality quantitative interpretation depends on disciplined workflow design rather than isolated processing steps improvements.

In a setting characterized by complex geology and orthogonal wide-azimuth acquisitions, achieving broadband fidelity required coordinated attention to wavelet stability, amplitude preservation, spatial regularization, and velocity accuracy throughout the processing chain.

Key contributors included joint source–receiver deghosting via 3D sparse τ–p inversion, AVO-guided demultiple, and controlled OVT regularization to enhance sampling while preserving geological integrity. Leveraging mask files and reciprocal OVT generation helped manage cross-survey data integration.

Depth imaging with TTI WE-KPSDM, ensured accurate positioning in areas of strong anisotropy and lateral velocity variation. Post-imaging refinements were implemented with strict amplitude control, allowing bandwidth enhancement and noise reduction while safeguarding low-frequency content and AVO behavior.

The final dataset delivers a stable platform for structural interpretation, AVO analysis, and inversion, and establishes a practical framework for broadband reprocessing in complex deepwater environments.

Acknowledgements

We extend our gratitude to bp and TGS for granting permission to publish this work.

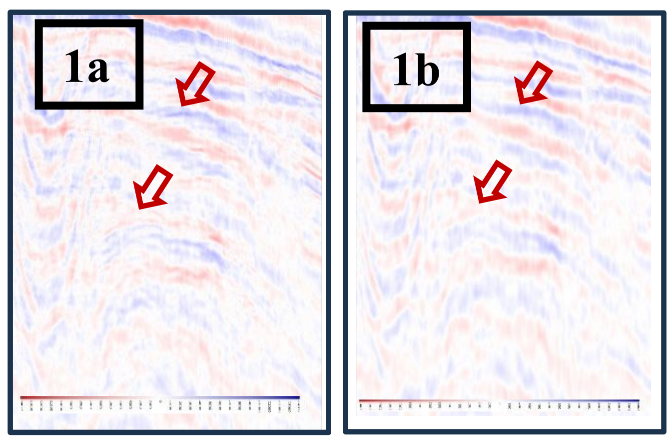

Figure 1a: Image domain QC demonstrating the SRME difference with primary leakage in the reservoir window. **1b:** Image domain QC demonstrating the SRME difference with no primary leakage in the reservoir window.

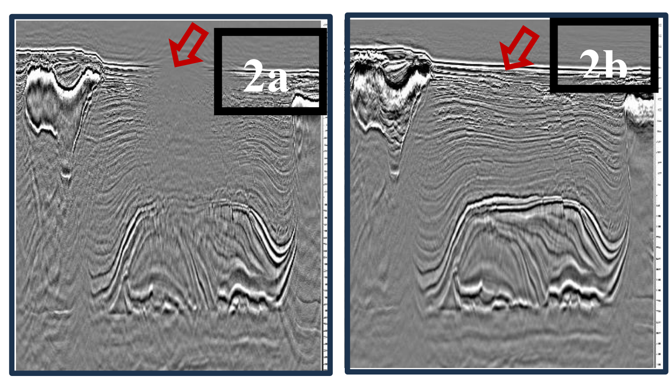

Figure 2a, 2b: Image domain QC demonstrating the effectiveness of reference-based 3D OVT regularization.

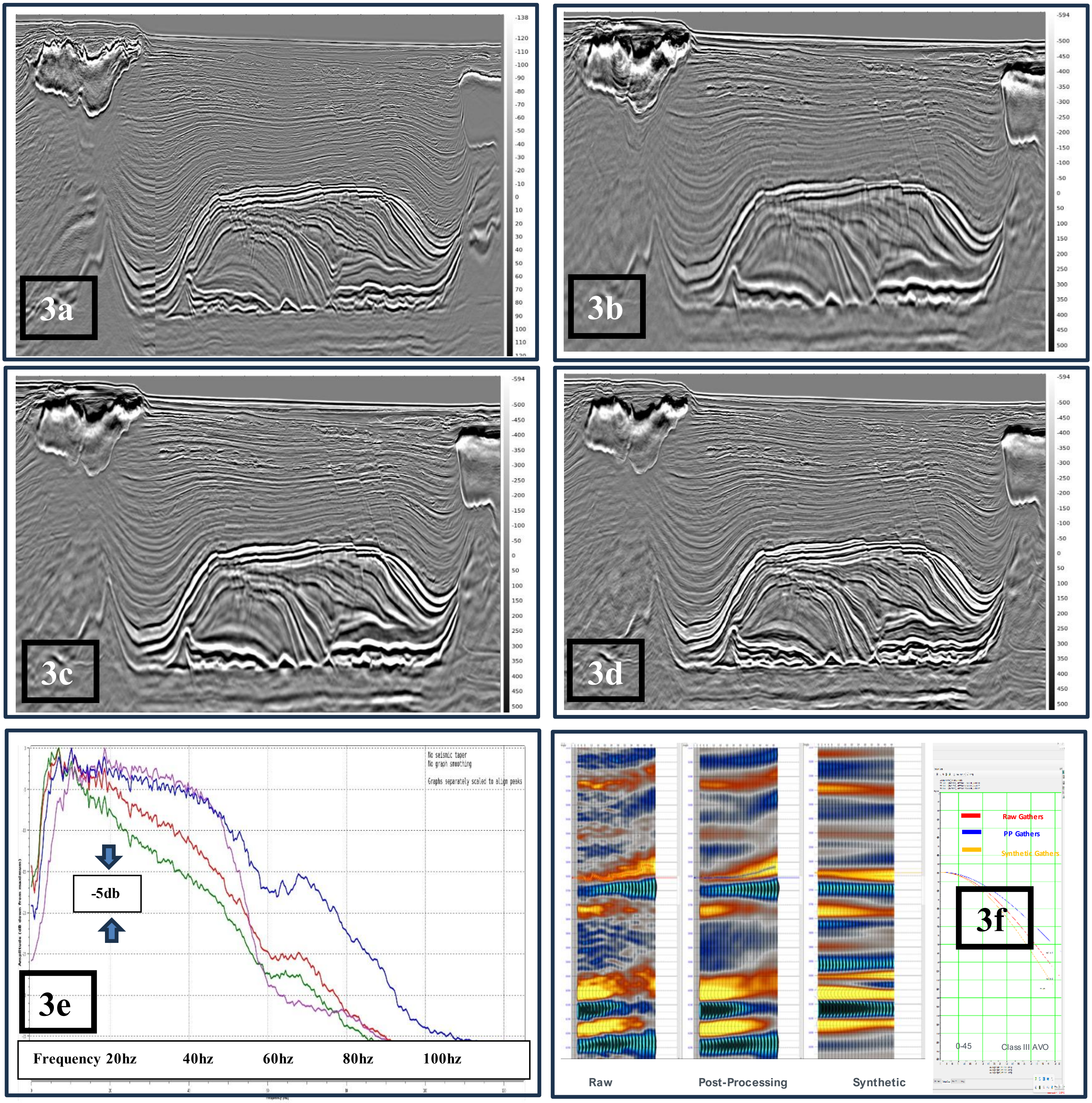

Figure 3a: Legacy LS WE-KPSDM image, generated using independently processed velocity models, separately merged. **3b:** Raw WE-KPSDM image produced using the merged velocity model. **3c:** WE-KPSDM image with Q = 150. **3d:** WE-KPSDM image with Q = 120. **3e:** Amplitude spectra comparison, where purple represents legacy data, green the raw WE-KPSDM result, red the Q = 150 result, and blue the Q = 120 result. **3f:** Post-processing of the image gathers maintained the overall AVO trend while improving signal-to-noise.

References:

Etgen, J. T., 2012, 3D wave equation Kirchhoff migration: 82nd Annual International Meeting, SEG, Expanded Abstracts

Mandroux, F., C.-O. Ting, B. Montgomery, and A. Lenart, 2013, Staggered marine acquisition design for complex imaging: SEG Technical Program Expanded Abstracts 2013, 26–30.

Pu, Y., G. Liu, D. Wang, H. Huang, and P. Wang, 2013, Wave-equation traveltime and amplitude for Kirchhoff migration: SEG Technical Program Expanded Abstracts 2013.

Regone, C., 2006, A modeling approach to wide-azimuth design for subsalt imaging: *The Leading Edge*, 25, no. 12, 1467–1475.

Wang, P., K. Nimsaila, D. Zhuang, Z. Fu, H. Shen, G. Poole, and N. Chazalnoel, 2015, Joint 3D source-side deghosting and designature for modern air-gun arrays: 77th EAGE Conference & Exhibition, Extended Abstracts.